Tunneling Transport of Unitary Fermions across the Superfluid Transition

G. Del Pace,[1,2,3,*] W. J. Kwon,[2,3] M. Zaccanti,[2,3] G. Roati,[2,3] and F. Scazza[2,3,†]
[1]Department of Physics and Astronomy, University of Florence, 50019 Sesto Fiorentino, Italy
[2]European Laboratory for Nonlinear Spectroscopy (LENS), 50019 Sesto Fiorentino, Italy
[3]Istituto Nazionale di Ottica del Consiglio Nazionale delle Ricerche (CNR-INO), 50019 Sesto Fiorentino, Italy

(Received 30 July 2020; accepted 12 January 2021; published 4 February 2021)

We investigate the transport of a Fermi gas with unitarity-limited interactions across the superfluid phase transition, probing its response to a direct current (dc) drive through a tunnel junction. As the superfluid critical temperature is crossed from below, we observe the evolution from a highly nonlinear to an Ohmic conduction characteristic, associated with the critical breakdown of the Josephson dc current induced by pair condensate depletion. Moreover, we reveal a large and dominant anomalous contribution to resistive currents, which reaches its maximum at the lowest attained temperature, fostered by the tunnel coupling between the condensate and phononic Bogoliubov-Anderson excitations. Increasing the temperature, while the zeroing of supercurrents marks the transition to the normal phase, the conductance drops considerably but remains much larger than that of a normal, uncorrelated Fermi gas tunneling through the same junction. We attribute such enhanced transport to incoherent tunneling of sound modes, which remain weakly damped in the collisional hydrodynamic fluid of unpaired fermions at unitarity.

DOI: 10.1103/PhysRevLett.126.055301

Quantum mechanical tunneling underlies many fundamental phenomena in physics, and it is the backbone for the operation of a variety of electronic devices, ranging from flash memories to SQUID magnetometers. A minimal realization of quantum tunneling is a so-called tunnel junction, created by connecting two conducting materials through a thin insulating layer or potential barrier [1]. Tunnel junctions represent a unique architecture to understand the elementary many-body mechanisms behind mesoscopic transport in quantum systems [1–3], hinging essentially on the nature of elementary excitations above the ground state [4]. In fermionic systems with attractive interactions, pairing correlations deeply affect both the equilibrium state and its low-energy excitations, leading to superfluidity when fermion pairs condense below the critical temperature. The excitation spectrum of fermion condensates incorporates both fermionic quasiparticles [5,6] and gapless Bogoliubov-Anderson (BA) phonons [6–9]. While the former correspond to pair-breaking excitations, the latter are associated with spontaneous symmetry breaking [10], and are essential for the condensate to acquire superfluid properties [11].

Whereas electron transport in superconducting tunnel junctions (STJs) is well understood within the Bardeen-Cooper-Schrieffer (BCS) regime of weak attractive interactions, where fermionic degrees of freedom govern both supercurrents and incoherent currents [12,13], a more intricate interplay between phononic and fermionic excitations is expected to arise in strongly attractive Fermi systems [8,9,14,15]. Atomic Fermi gases near a Feshbach resonance provide a well-controlled framework for addressing two-terminal transport in strongly interacting quantum fluids [16], allowing one to reach the universal, unitarity-limited interaction regime [9]. In particular, resonant Fermi gases represent the most robust known instance of fermionic superfluidity, and feature hydrodynamic behavior even in the normal phase [17–19]. This has spurred experimental investigations of mesoscopic transport in unitary superfluid junctions [20–26], which have revealed nonlinear current-bias characteristics from multiple Andreev reflections [22] or Josephson supercurrents [25].

In this work, we explore the tunneling conduction of a resonant atomic Fermi gas across the superfluid transition. We show that both supercurrents and normal currents react distinctly to the temperature, as they are tied to the amplitude of the superfluid order parameter—the pair condensate density—and to its excitation modes. In particular, by measuring the response to a tunable direct current (dc) drive I_{ext} in a tunnel junction at varying temperature T, we observe the critical breakdown of coherent Josephson transport. The dependence of the maximum supercurrent $I_{s,\mathrm{max}}$ on the temperature is captured by a theoretical model relying on the thermal depletion of the condensate density, which vanishes at the critical temperature T_c. Further, we reveal a large anomalous contribution to the bias-independent conductance, dominating the resistive current branch arising for $|I_{\mathrm{ext}}| > I_{s,\mathrm{max}}$ at low temperatures, which we ascribe to the conversion of the condensate into phononic BA modes. Being fueled by the condensate, unlike quasiparticle currents in STJs, the ensuing normal current decreases

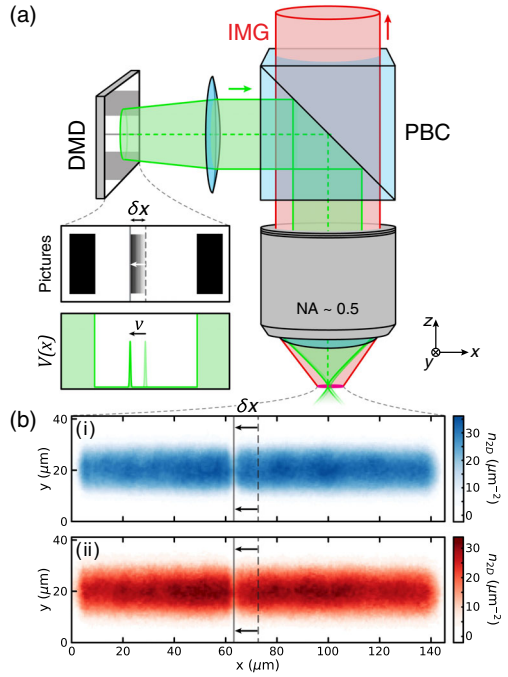

FIG. 1. A current-driven tunnel junction between resonant Fermi gases across the superfluid transition. (a) Experimental realization of a tunneling dc drive by dynamical optical potentials. The surface of a DMD displaying the junction geometry, composed of a central barrier and two end caps, is projected onto the atoms through a NA $\simeq 0.5$ objective, creating a repulsive potential $V(\mathbf{r})$. The barrier is set in uniform motion at velocity v by playing a sequence of images on the DMD at the desired frame rate, and is swept over a distance δx along the x axis. (b) *In situ* absorption images of the atomic density at unitarity, acquired immediately after completing a $\delta x \simeq 10$ μm barrier translation. The column-integrated density profiles $n_{2D}(x, y)$ are shown for an injected current $I_{\text{ext}} \simeq 3.9 \times 10^5$ s^{-1} at (i) $T = 0.08(1)T_F$ and (ii) $T = 0.18(1)T_F$. While no density difference is visible between the two reservoirs for the colder sample, the hotter one displays a density increase in the left reservoir, producing a chemical potential bias $\Delta\mu \neq 0$ across the junction.

towards T_c, above which broken pairs are expected to eventually become the dominant current carriers. Indeed, by measuring the scaling of conductance with the tunneling barrier strength, we distinguish conduction mediated by paired or unpaired fermions. Yet, for $T \gtrsim T_c$ the conductance remains much larger than that measured in a metallic state, even though BA phonons cannot propagate in the absence of the order parameter. We ascribe this to incoherent tunneling of hydrodynamic sound modes, stabilized by elastic collisions between unpaired fermions. Our measurements support scenarios where no significant preformed pair fraction exists at unitarity above T_c [27–29].

In our experiment, two tunnel-coupled, strongly interacting atomic reservoirs are created by confining a Feshbach-resonant Fermi gas into a hybrid optical potential, combining a harmonic optical trap with repulsive potentials tailored by a digital micromirror device (DMD). Each reservoir contains approximately $N_{R,L} \simeq 4 \times 10^4$ atoms in each of the two lowest hyperfine states of ^{6}Li. The reservoirs are set initially in thermochemical equilibrium, and their temperature is adjusted between $T/T_F = 0.07(1)$ and $0.23(1)$, across the superfluid transition for unitarity-limited interactions at $T_c \simeq 0.21T_F$ [29,30]. Here, E_F and $T_F = E_F/k_B$ are the in-trap Fermi energy and temperature [31]. The optical setup for creating and driving the tunnel junction is illustrated in Fig. 1(a). The reservoirs are separated by a thin, repulsive optical barrier, which is Gaussian along the x direction with a $1/e^2$ width $w_0 \simeq 0.95(9)$ μm and nearly homogeneous along the y and z direction [25,31]. Its intensity profile and position are controlled by the DMD, whose surface is imaged onto the atomic sample through a high-resolution objective, creating also two sharp axial end caps. To initialize the junction, the barrier is adiabatically raised at the trap center to the target potential height V_0 experienced by one fermion. This creates two identical reservoirs with vanishing relative imbalance $z = (N_L - N_R)/N \simeq 0$, and correspondingly vanishing chemical potential difference $\Delta\mu = \mu_L - \mu_R \simeq 0$, where $N = N_L + N_R$ and $\mu_{R,L}$ are the fermion chemical potentials in the reservoirs. To probe the response of the junction to an external dc drive, we set the potential barrier in uniform motion with respect to the gas [25,45,46]. The imparted current I_{ext} is proportional to the barrier velocity v, and for a constant total barrier displacement $\delta x \simeq 10$ μm, $I_{\text{ext}} = -\bar{z}N/2 \times |v|/\delta x$, where $\bar{z} \simeq \pm 0.15$ is the relative imbalance at equilibrium for the final barrier position $x = \pm\delta x$. By measuring the relative imbalance z after the barrier displacement via *in situ* absorption imaging [see Fig. 1(b)], we determine the induced potential difference $\Delta\mu = (z - \bar{z})E_c N/2$. Here, $E_c = 2\partial\mu_L/\partial N_L$ (calculated with $N_L = N/2$) is the effective charging energy of the junction, that is the inverse compressibility of the reservoirs quantifying their density response to currents [14,45].

In a full measurement at fixed temperature, we obtain $\Delta\mu$ as a function of I_{ext}, corresponding to the "current-voltage" I-$\Delta\mu$ response of the junction [25]. Figure 2(a) illustrates the effect of reservoir temperature on such response at unitarity. At low temperature, the junction exhibits $\Delta\mu \simeq 0$ for $|I_{\text{ext}}| \leq I_{s,\max}$, implying vanishing resistance below a maximum current $I_{s,\max}$. By raising the temperature, smaller values of I_{ext} suffice to yield a finite $|\Delta\mu| > 0$. Eventually, $I_{s,\max}$ vanishes and any nonzero applied current produces a chemical potential difference, hence the junction becomes fully resistive. Crucially, the junction crosses over from a nonlinear to an Ohmic current-potential characteristic, reflecting the phase transition of the system from the superfluid to the normal state [13,47,48]. Within the linear response regime $\Delta\mu \ll \mu_0$ explored here, where μ_0 is the peak chemical potential in the absence of barrier, the current injected through the junction can be decomposed as [13,48]

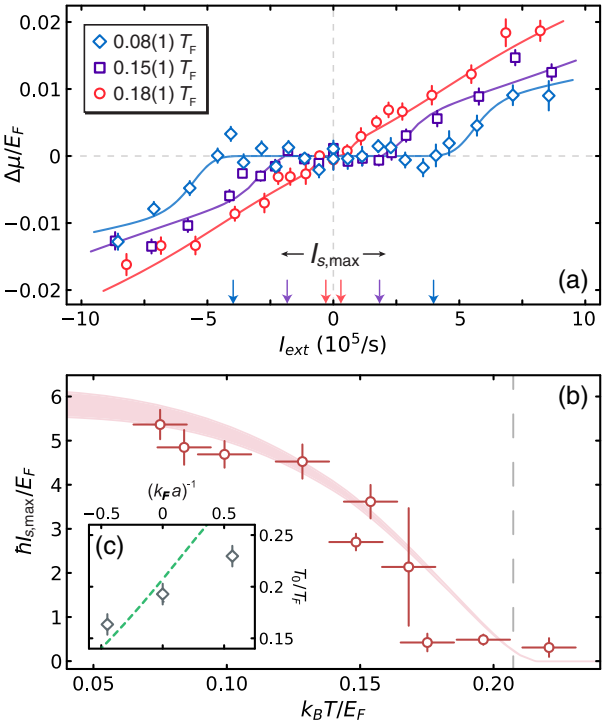

FIG. 2. Breakdown of dc tunneling supercurrents in strongly interacting Fermi gases. (a) Current-potential I-$\Delta\mu$ characteristics of the junction at unitarity for different gas temperatures T/T_F (see legend). Solid lines represent fits of experimental data with a RCSJ circuit model [31]. The fitted values for the maximum supercurrent $I_{s,\max}$ are denoted by arrows on the bottom axis. Error bars denote the standard deviation of the mean (s.e.m.) from averaging over ~10 experimental realizations. (b) $I_{s,\max}$ at unitarity as a function of the reduced temperature T/T_F. Vertical (horizontal) error bars combine the standard error on $I_{s,\max}$ (temperature) with statistical errors from averaging typically two independent extractions. The shaded region indicates the calculated $I_{s,\max}$ (see text), considering a 10% uncertainty around the nominal barrier width and a 3.5% uncertainty on the calculated E_F. The barrier height is fixed at $V_0/\mu_0 \simeq 0.7$, where $\mu_0 \approx 0.6E_F$ [50]. The dashed vertical line marks the predicted critical temperature T_c for the superfluid transition at unitarity [30]. (c) Critical temperature T_0/T_F for the disappearance of Josephson currents as a function of interaction strength $(k_Fa)^{-1}$. Experimental results are compared with the theoretically obtained T_c from Ref. [29] (green dashed line).

$$I_{\rm ext} = I_s(\varphi) + G\Delta\mu + C\Delta\dot{\mu}, \tag{1}$$

where $\varphi = \varphi_L - \varphi_R$ is the phase difference between the pair condensates in the reservoirs, $I_s(\varphi)$ is the current-phase relation of the junction, G is the bias-independent tunneling conductance, and $C = 1/E_c$ is the effective junction capacitance. For barrier heights $V_0/\mu_0 \sim 1$, corresponding to small junction transmissions $|t_p|^2 \ll 1$, where t_p is the tunneling amplitude of a single pair, one can retain only the first two orders in the tunnel coupling [14,25] such that $I_s(\varphi) \simeq I_1 \sin\varphi + I_2 \sin 2\varphi$, where the coefficients I_n are of order $|t_p|^n$ [14,49]. In the absence of an initial bias potential, $I_{s,\max} = \max_{\varphi\in[0,\pi)} |I_s(\varphi)|$ sets the largest value of $I_{\rm ext}$ for which the junction exhibits zero normal current, i.e., $\Delta\mu = 0$ for $|I_{\rm ext}| \le I_{s,\max}$. The observed zero-potential plateaus [see Fig. 2(a)] gauge therefore the maximum Josephson supercurrent flowing through the junction [25], which vanishes for $T \ge T_c$ in the normal state. On the other hand, the charging rate GE_c sets the timescale for the junction resistive response. Combining Eq. (1) with the Josephson-Anderson relation $\hbar\dot{\varphi} = -\Delta\mu$ yields the resistively and capacitively shunted junction (RCSJ) circuit model, widely applied to STJs [48]. To characterize the junction response, we fit the measured I-$\Delta\mu$ curves with the numerical solution of such a RCSJ model [31], extracting $I_{s,\max}$ and G for each temperature.

Figure 2(b) shows the obtained $I_{s,\max}$ at unitarity as a function of the reservoir temperature. The observed trend resembles that predicted within BCS theory by the Ambegaokar-Baratoff (AB) formula, $I_{s,\max} = \pi\Delta/2 \times G_n \tanh(\Delta/2k_BT)$ [51], where Δ is the superconducting gap, and G_n is the conductance of the junction in the normal state right above T_c, set essentially by the single-fermion tunneling probability. However, the weak-coupling AB result is not expected to hold at strong interactions, even for $T = 0$ [52,53]. Therefore, we model our system by generalizing to finite temperatures the effective theory presented in Refs. [25,53], where the Josephson supercurrent is explicitly linked to the condensate density, obtaining the shaded curve in Fig. 2(b) [31]. For this, we exploit Luttinger-Ward calculations of the condensate fraction for a homogeneous unitary Fermi gas [54], as well as its equation of state [50] in the local density approximation (LDA). With no free parameters, the model quantitatively reproduces the experimental data, evidencing a firm connection between $I_{s,\max}$ and the condensate density at any temperature. Yet, some discrepancy appears when approaching T_c. While the calculated $I_{s,\max}$ vanishes essentially at T_c [dashed vertical line Fig. 2(b)], the measured one sharply drops to nearly zero already at $T_0 < T_c$. Such deviation could result from the radial inhomogeneity of the gas, causing different shells to undergo the superfluid transition at different T. Furthermore, a finite $\Delta\mu$ at $T < T_c$ could develop from thermal fluctuations in the superfluid state [47,55]. In particular, stochastic thermal phase slips, whose probability scales as $\exp(-2\hbar I_{s,\max}/k_BT)$ [55], are expected to become relevant when $\hbar I_{s,\max} \lesssim E_F$, which in our system occurs at $T \gtrsim 0.17T_F$. We determine the critical temperature T_0 for the breakdown of Josephson supercurrents through a piecewise function fit of $I_{s,\max}(T)$ [31]. At unitarity $T_0 = 0.19(1)T_F$, consistent with what is expected from thermal phase slips, but also with the value $T_c = 0.21(1)T_F$ predicted by the Luttinger-Ward technique [30] within their respective uncertainties. The same procedure is used to determine T_0 at different interaction strengths, parametrized by $(k_Fa)^{-1}$ where $k_F = \sqrt{2mE_F}/\hbar$ and a is

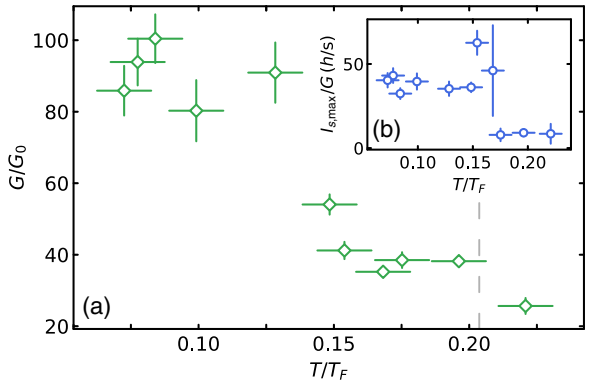

FIG. 3. Bias-independent tunneling conductance G as a function of T/T_F, measured at unitarity under the same experimental conditions of Fig. 2. (a) G is normalized to the conductance per spin component $G_0 = 102(15)h^{-1}$ of a noninteracting Fermi gas, measured at $T = 0.21(1)T_F$ with an equivalent barrier height $V_0/\mu_0 \simeq 0.73$. Vertical (horizontal) error bars combine the standard error on the extracted conductance (temperature) with statistical errors from averaging typically two independent extractions. The dashed vertical line locates the theoretical critical temperature T_c at unitarity [30]. (b) Experimentally obtained $I_{s,\max}/G$ as a function of T/T_F.

the s-wave scattering length, as displayed in Fig. 2(c). The observed monotonic increase of T_0 from negative to positive couplings reflects that of the superfluid critical temperature T_c [9,29].

The bias-independent tunneling conductance G obtained at unitarity is shown in Fig. 3(a) as a function of temperature, normalized to the measured (normal-state) conductance $G_0 = 102(15)h^{-1}$ of a noninteracting Fermi gas. G increases monotonically with decreasing T, taking values as large as $G \sim 10^2 G_0 \sim 10^4 h^{-1}$, and greatly exceeds G_0 for any T. We compute the normal-state conductance of the junction considering zero-temperature ideal fermionic reservoirs within the LDA [31], obtaining $G_n = 160(29)h^{-1}$, in reasonable agreement with the measured G_0. The mismatch between the measured G and G_0 (or the estimated G_n) indicates that normal currents in our neutral gas junction do not arise from incoherent pair or quasiparticle tunneling, but rather from collective bosonic excitations [15,23]. In the small bias regime at low temperature $\Delta\mu \ll \Delta$, broken pairs are energetically suppressed as $\exp(-\Delta/k_B T)$, and the only accessible excitations out of the condensate are gapless low-momentum BA phonons [8,17]. Only at $T \sim T_c$, fermionic quasiparticles proliferate, and their incoherent tunneling may take over as the main conduction mechanism. Conversely, pair-breaking processes in STJs typically determine both the maximum Josephson supercurrent and normal tunneling current [13], while no key role is played by BA phonons that are lifted into gapped plasmons by the Coulomb repulsion [7].

A phononic contribution to the dc conductance, arising from the tunnel coupling between the condensate in one reservoir and sound modes in the other, has indeed been predicted both for weakly interacting BECs [14] and recently for neutral fermionic superfluids in the BCS regime [15]. Such *anomalous* contribution is maximum at $T = 0$, being fostered by the condensate and its gapless phononic excitations. Additionally, a *normal* contribution to the conductance is expected from incoherent tunneling of phononic excitations, whose population does not vanish at $T = 0$ owing to quantum depletion, and grows as $\sim T^4$ at low temperatures [9,14]. While a full description of tunneling transport at unitarity remains an open theoretical challenge, fermionic quasiparticle transport appears essentially irrelevant with respect to the experimentally obtained conductance, which provides strong evidence for anomalous tunneling currents in unitary superfluids. The anomalous character of the low-temperature conductance is further confirmed by extracting the ratio $I_{s,\max}/G$ [see Fig. 3(b)]. Whereas in STJs this quantifies the superconducting gap via the AB formula [13,51], the approximately constant value observed here until nearby T_0 demonstrates the tight relation between G and the condensate density. As the temperature approaches T_c, the anomalous term is expected to extinguish its effect, and significant incoherent tunneling should set in. However, unlike collisionless gases where fermionic quasiparticles are the only available excitations above T_c, our strongly interacting fluid supports weakly damped hydrodynamic sound even in the normal phase, with no distinct signature emerging at low momenta across the superfluid transition [18,19]. Therefore, phonon tunneling is not expected to fade at T_c, explaining the observed trend of G: despite dropping by nearly an order of magnitude from its maximum, G remains much larger than G_0 also for $T \gtrsim T_c$.

The tunnel conductance also provides information about the nature of current carriers, being sensitive to whether transport is mediated by pairs or unpaired fermions. In the absence of pair breaking, resistive currents arise only at second order in the tunnel coupling between pairs in the reservoirs [14,56], namely $G \propto |t_p|^2$. We directly confirm this scaling by comparing the conductance and the supercurrent amplitude at varying barrier strength, finding $G^{1/2} \propto I_{s,\max} \sim |t_p|$ at low temperature [inset of Fig. 4(a)]. On the other hand, when broken pairs prevail, G should reflect the single-fermion tunneling probability $|t_F|^2$, namely $G \propto |t_F|^2$. In the tunneling limit, both $|t_p|$ and $|t_F|$ decrease exponentially with the adimensional barrier strength $\eta_b = k_F d\sqrt{V_0/E_F}$, $d = 0.6 w_0$ being the effective barrier size [31]. Yet, one can show that $\log|t_p| \approx 2\log|t_F|$, when accounting for the different mass and polarizability of bound pairs and unpaired atoms [31]. Figures 4(a)–4(c) compare the measured scaling of the charging rate GE_c with η_b, for three distinct regimes across the superfluid transition. In all regimes, we observe indeed that $\log GE_c \propto -\eta_b$. Remarkably, a unitary gas at $T \simeq T_c$ [panel (b)] exhibits a weaker dependence of GE_c on η_b than a unitary superfluid at $T \simeq 0.3T_c$ [panel (a)], whereas its

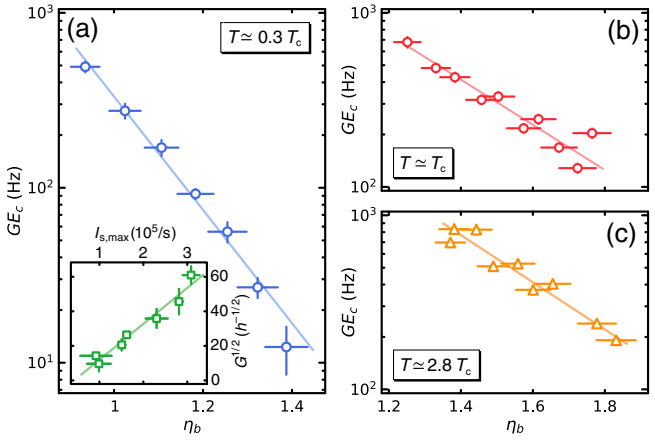

FIG. 4. Charging rate GE_c as a function of the adimensional barrier strength $\eta_b = (k_F d) \times \sqrt{V_0/E_F}$ [31] for (a) a superfluid unitary gas at $T = 0.06(1)T_F \simeq 0.3T_c$, (b) a unitary gas at $T = 0.20(1)T_F \simeq T_c$, and (c) a normal attractive Fermi gas with $(k_F a)^{-1} \simeq -0.82$ at $T = 0.20(1)T_F \simeq 2.8T_c$ [61]. In panel (a), $E_F/h \simeq 6$ kHz (data taken from Ref. [25]), while $E_F/h \simeq 11$ kHz in panel (b) and (c). Vertical and horizontal error bars result from the standard error on G and the experimental uncertainty on V_0, respectively. Solid lines represent linear fits of $\log GE_c$. In the inset of panel (a), the measured $G^{1/2}$ and $I_{s,\max}$ are compared within the same η_b range.

behavior matches that of a normal attractive Fermi gas at $T > T_c$ [panel (c)]. Performing linear fits of $\log GE_c$, we find a ratio of 2.5(3) between the slopes in the superfluid and critical unitary regimes, nearly compatible with the factor 2 expected between tightly bound pairs and free fermions. Such observations point to a distinctive change of resistive-current carriers from pairs to single fermionic quasiparticles, upon crossing T_c from below. Further, our measurements suggest that for $T \simeq 0.20T_F$ incoherent transport at unitarity is dominated by unpaired fermions, although weak "pseudogap" correlations [29,57–59], to which low-momentum phonons are essentially insensitive [19], may exist—and could be probed through spin conductance [60].

In conclusion, we have demonstrated that tunneling currents constitute a powerful probe of the superfluid order parameter of unitary fermions at finite temperatures, providing a striking signature of the superfluid phase transition [50,62,63]. The order parameter is found to impact both zero-resistance and Ohmic conduction, feeding Josephson and anomalous normal currents, hence highlighting significant differences between transport in neutral and charged quantum fluids. We anticipate the observed anomalous low-resistance conduction to be a generic feature, not restricted to the large-area, multimode junction used here, as suggested by recent theoretical investigations of weakly interacting neutral superfluids at quantum point contacts [15,56]. In the future, it will be interesting to focus on the regime $T \simeq T_c$, where thermally activated phase slips modify the current-potential characteristics [47,55] and conduction may be influenced by pairing fluctuations [28,64,65]. The anomalous and normal contributions to Ohmic currents could be disentangled by measuring heat transport [15,24,56]. Finally, realizing a spin-current drive within the same tunneling geometry will enable us to probe fermion correlations in the pseudogap regime [60].

We are indebted to Jean-Philippe Brantut, Eugene Demler, Tilman Enss, Carlos Sa De Melo, Verdiana Piselli, Giancarlo Strinati, Wilhelm Zwerger, and Massimo Inguscio for inspiring discussions. We thank Bernhard Frank for providing us with finite-temperature Luttinger-Ward calculations of the condensed fraction of the homogeneous unitary Fermi gas, Michele Pini for providing us with self-consistent calculations of the critical temperature, and Riccardo Panza for assistance during the construction of the experimental setup. This work was supported by the European Research Council under GA No. 307032, Ente Cassa di Risparmio di Firenze Project No. 2016.0770, the Italian MIUR under the PRIN2017 project CEnTraL, and EU's Horizon 2020 research and innovation programme under the Qombs project FET Flagship on Quantum Technologies GA No. 820419, and Marie Skłodowska-Curie GAs No. 705269 and No. 843303.

*delpace@lens.unifi.it
†scazza@lens.unifi.it

[1] *Tunneling Phenomena in Solids*, edited by E. Burstein and S. Lundqvist (Springer, Boston, MA, 1969).
[2] I. Giaever, Energy Gap in Superconductors Measured by Electron Tunneling, Phys. Rev. Lett. **5**, 147 (1960).
[3] S. Datta, *Electronic Transport in Mesoscopic Systems* (Cambridge University Press, Cambridge, England, 1997).
[4] D. Pines and P. Noziéres, *Theory of Quantum liquids*, Vol. 1 (Perseus Books Publishing, Cambridge, MA, 1999).
[5] S. A. Kivelson and D. S. Rokhsar, Bogoliubov quasiparticles, spinons, and spin-charge decoupling in superconductors, Phys. Rev. B **41**, 11693 (1990).
[6] N. N. Bogoliubov, V. V. Tolmachov, and D. V. Širkov, A new method in the theory of superconductivity, Fortschr. Phys. **6**, 605 (1958).
[7] P. W. Anderson, Random-phase approximation in the theory of superconductivity, Phys. Rev. **112**, 1900 (1958).
[8] R. Combescot, M. Y. Kagan, and S. Stringari, Collective mode of homogeneous superfluid Fermi gases in the BEC-BCS crossover, Phys. Rev. A **74**, 042717 (2006).
[9] *The BCS-BEC Crossover and the Unitary Fermi Gas*, edited by W. Zwerger (Springer, Berlin-Heidelberg, 2012), Vol. 836.
[10] J. Goldstone, Field theories with superconductor solutions, Nuovo Cimento **19**, 154 (1961).
[11] L. Landau, Theory of the superfluidity of helium II, Phys. Rev. **60**, 356 (1941).
[12] G. E. Blonder, M. Tinkham, and T. M. Klapwijk, Transition from metallic to tunneling regimes in superconducting

microconstrictions: Excess current, charge imbalance, and supercurrent conversion, Phys. Rev. B **25**, 4515 (1982).
[13] M. Tinkham, *Introduction to Superconductivity*, 2nd ed. (McGraw-Hill, New York, 1996).
[14] F. Meier and W. Zwerger, Josephson tunneling between weakly interacting Bose-Einstein condensates, Phys. Rev. A **64**, 033610 (2001).
[15] S. Uchino, Role of Nambu-Goldstone modes in the fermionic-superfluid point contact, Phys. Rev. Research **2**, 023340 (2020).
[16] S. Krinner, T. Esslinger, and J.-P. Brantut, Two-terminal transport measurements with cold atoms, J. Phys. Condens. Matter **29**, 343003 (2017).
[17] S. Hoinka, P. Dyke, M. G. Lingham, J. J. Kinnunen, G. M. Bruun, and C. J. Vale, Goldstone mode and pair-breaking excitations in atomic Fermi superfluids, Nat. Phys. **13**, 943 (2017).
[18] C. C. N. Kuhn, S. Hoinka, I. Herrera, P. Dyke, J. J. Kinnunen, G. M. Bruun, and C. J. Vale, High-Frequency Sound in a Unitary Fermi Gas, Phys. Rev. Lett. **124**, 150401 (2020).
[19] P. B. Patel, Z. Yan, B. Mukherjee, R. J. Fletcher, J. Struck, and M. W. Zwierlein, Universal sound diffusion in a strongly interacting Fermi gas, Science **370**, 1222 (2020).
[20] D. Stadler, S. Krinner, J. Meineke, J.-P. Brantut, and T. Esslinger, Observing the drop of resistance in the flow of a superfluid Fermi gas, Nature (London) **491**, 736 (2012).
[21] G. Valtolina, A. Burchianti, A. Amico, E. Neri, K. Xhani, J. A. Seman, A. Trombettoni, A. Smerzi, M. Zaccanti, M. Inguscio, and G. Roati, Josephson effect in fermionic superfluids across the BEC-BCS crossover, Science **350**, 1505 (2015).
[22] D. Husmann, S. Uchino, S. Krinner, M. Lebrat, T. Giamarchi, T. Esslinger, and J.-P. Brantut, Connecting strongly correlated superfluids by a quantum point contact, Science **350**, 1498 (2015).
[23] A. Burchianti, F. Scazza, A. Amico, G. Valtolina, J. A. Seman, C. Fort, M. Zaccanti, M. Inguscio, and G. Roati, Connecting Dissipation and Phase Slips in a Josephson Junction Between Fermionic Superfluids, Phys. Rev. Lett. **120**, 025302 (2018).
[24] D. Husmann, M. Lebrat, S. Häusler, J.-P. Brantut, L. Corman, and T. Esslinger, Breakdown of the Wiedemann–Franz law in a unitary Fermi gas, Proc. Natl. Acad. Sci. U.S.A. **115**, 8563 (2018).
[25] W. J. Kwon, G. Del Pace, R. Panza, M. Inguscio, W. Zwerger, M. Zaccanti, F. Scazza, and G. Roati, Strongly correlated superfluid order parameters from dc Josephson supercurrents, Science **369**, 84 (2020).
[26] N. Luick, L. Sobirey, M. Bohlen, V. P. Singh, L. Mathey, T. Lompe, and H. Moritz, An ideal Josephson junction in an ultracold two-dimensional Fermi gas, Science **369**, 89 (2020).
[27] B. Jankó, I. Kosztin, K. Levin, M. R. Norman, and D. J. Scalapino, Incoherent Pair Tunneling as a Probe of the Cuprate Pseudogap, Phys. Rev. Lett. **82**, 4304 (1999).
[28] N. Bergeal, J. Lesueur, M. Aprili, G. Faini, J. P. Contour, and B. Leridon, Pairing fluctuations in the pseudogap state of copper-oxide superconductors probed by the Josephson effect, Nat. Phys. **4**, 608 (2008).
[29] M. Pini, P. Pieri, M. Jaeger, J. P. H. Denschlag, and G. Strinati, Pair correlations in the normal phase of an attractive Fermi gas, New J. Phys. **22**, 083008 (2020).
[30] R. Haussmann and W. Zwerger, Thermodynamics of a trapped unitary Fermi gas, Phys. Rev. A **78**, 063602 (2008).
[31] See Supplemental Material at http://link.aps.org/supplemental/10.1103/PhysRevLett.126.055301, which includes Refs. [32–44], for details on the experimental methods and the theoretical modeling tools.
[32] K. Xhani, E. Neri, L. Galantucci, F. Scazza, A. Burchianti, K.-L. Lee, C. F. Barenghi, A. Trombettoni, M. Inguscio, M. Zaccanti, G. Roati, and N. P. Proukakis, Critical Transport and Vortex Dynamics in a Thin Atomic Josephson Junction, Phys. Rev. Lett. **124**, 045301 (2020).
[33] W. Ketterle and M. W. Zwierlein, Making, probing and understanding ultracold Fermi gases, in *Ultra-cold Fermi gases, in Proceedings of the International School of Physics "Enrico Fermi,"* Vol. 164, edited by M. Inguscio, W. Ketterle, and C. Salomon (IOS press, Amsterdam, 2008), pp. 95–287.
[34] E. R. S. Guajardo, M. K. Tey, L. A. Sidorenkov, and R. Grimm, Higher-nodal collective modes in a resonantly interacting Fermi gas, Phys. Rev. A **87**, 063601 (2013).
[35] X.-J. Liu, H. Hu, and P. D. Drummond, Virial Expansion for a Strongly Correlated Fermi Gas, Phys. Rev. Lett. **102**, 160401 (2009).
[36] S. Nascimbène, N. Navon, K. J. Jiang, F. Chevy, and C. Salomon, Exploring the thermodynamics of a universal Fermi gas, Nature (London) **463**, 1057 (2010).
[37] E. Taylor, H. Hu, X.-J. Liu, L. P. Pitaevskii, A. Griffin, and S. Stringari, First and second sound in a strongly interacting Fermi gas, Phys. Rev. A **80**, 053601 (2009).
[38] Y.-H. Hou, L. P. Pitaevskii, and S. Stringari, First and second sound in a highly elongated Fermi gas at unitarity, Phys. Rev. A **88**, 043630 (2013).
[39] J. E. Thomas, J. Kinast, and A. Turlapov, Virial Theorem and Universality in a Unitary Fermi Gas, Phys. Rev. Lett. **95**, 120402 (2005).
[40] L. D. Carr, G. V. Shlyapnikov, and Y. Castin, Achieving a BCS Transition in an Atomic Fermi Gas, Phys. Rev. Lett. **92**, 150404 (2004).
[41] S. Eckel, J. G. Lee, F. Jendrzejewski, C. J. Lobb, G. K. Campbell, and W. T. Hill, Contact resistance and phase slips in mesoscopic superfluid-atom transport, Phys. Rev. A **93**, 063619 (2016).
[42] R. E. Prange, Tunneling from a many-particle point of view, Phys. Rev. **131**, 1083 (1963).
[43] D. ter Haar, *Problems in Quantum Mechanics*, 3rd ed. (Pion Limited, London, 1975).
[44] E. Goldobin, D. Koelle, R. Kleiner, and A. Buzdin, Josephson junctions with second harmonic in the current-phase relation: Properties of φ junctions, Phys. Rev. B **76**, 224523 (2007).
[45] S. Giovanazzi, A. Smerzi, and S. Fantoni, Josephson Effects in Dilute Bose-Einstein Condensates, Phys. Rev. Lett. **84**, 4521 (2000).

[46] S. Levy, E. Lahoud, I. Shomroni, and J. Steinhauer, The a.c. and d.c. Josephson effects in a Bose–Einstein condensate, Nature (London) **449**, 579 (2007).
[47] J. T. Anderson and A. M. Goldman, Thermal Fluctuations and the Josephson Supercurrent, Phys. Rev. Lett. **23**, 128 (1969).
[48] A. Barone and G. Paternò, *Physics and Applications of the Josephson Effect* (John Wiley, New York, 1982).
[49] F. Bloch, Josephson Effect in a Superconducting Ring, Phys. Rev. B **2**, 109 (1970).
[50] M. J. H. Ku, A. T. Sommer, L. W. Cheuk, and M. W. Zwierlein, Revealing the Superfluid Lambda Transition in the Universal Thermodynamics of a Unitary Fermi Gas, Science **335**, 563 (2012).
[51] V. Ambegaokar and A. Baratoff, Tunneling Between Superconductors, Phys. Rev. Lett. **11**, 104 (1963).
[52] A. Spuntarelli, P. Pieri, and G. C. Strinati, Josephson Effect Throughout the BCS-BEC Crossover, Phys. Rev. Lett. **99**, 040401 (2007).
[53] M. Zaccanti and W. Zwerger, Critical Josephson current in BCS-BEC–crossover superfluids, Phys. Rev. A **100**, 063601 (2019).
[54] R. Haussmann, W. Rantner, S. Cerrito, and W. Zwerger, Thermodynamics of the BCS-BEC crossover, Phys. Rev. A **75**, 023610 (2007).
[55] B. I. Halperin, G. Refael, and E. Demler, Resistance in superconductors, Int. J. Mod. Phys. B **24**, 4039 (2010).
[56] S. Uchino and J.-P. Brantut, Bosonic superfluid transport in a quantum point contact, Phys. Rev. Research **2**, 023284 (2020).
[57] R. Haussmann, M. Punk, and W. Zwerger, Spectral functions and rf response of ultracold fermionic atoms, Phys. Rev. A **80**, 063612 (2009).
[58] P. Magierski, G. Wlazłowski, A. Bulgac, and J. E. Drut, Finite-Temperature Pairing Gap of a Unitary Fermi Gas by Quantum Monte Carlo Calculations, Phys. Rev. Lett. **103**, 210403 (2009).
[59] S. Jensen, C. N. Gilbreth, and Y. Alhassid, The pseudogap regime in the unitary Fermi gas, Eur. Phys. J. Spec. Top. **227**, 2241 (2019).
[60] Y. Sekino, H. Tajima, and S. Uchino, Mesoscopic spin transport between strongly interacting Fermi gases, Phys. Rev. Res. **2**, 023152 (2020).
[61] L. P. Gor'kov and T. K. Melik-Barkhudarov, Contribution to the theory of superfluidity in an imperfect Fermi gas, Sov. Phys. JETP **13**, 1018 (1961).
[62] S. Riedl, E. R. S. Guajardo, C. Kohstall, J. H. Denschlag, and R. Grimm, Superfluid quenching of the moment of inertia in a strongly interacting Fermi gas, New J. Phys. **13**, 035003 (2011).
[63] L. A. Sidorenkov, M. K. Tey, R. Grimm, Y.-H. Hou, L. Pitaevskii, and S. Stringari, Second sound and the superfluid fraction in a Fermi gas with resonant interactions, Nature (London) **498**, 78 (2013).
[64] D. J. Scalapino, Pair Tunneling as a Probe of Fluctuations in Superconductors, Phys. Rev. Lett. **24**, 1052 (1970).
[65] J. T. Anderson and A. M. Goldman, Experimental Determination of the Pair Susceptibility of a Superconductor, Phys. Rev. Lett. **25**, 743 (1970).